from partonic degrees of freedom to freeze-out

S.A. Bass[1]

Department of Physics

Duke University

Durham, NC, 27708-0305, USA

H. Weber, C. Ernst, M. Bleicher, M. Belkacem[2], L. Bravina[2], S. Soff, H. Stöcker and W. Greiner

Institut für Theoretische Physik

Johann Wolfgang Goethe Universität

Robert Mayer Str. 8-10

D-60054 Frankfurt am Main, Germany

C. Spieles[1]

Lawrence Berkeley Laboratory

1 Cyclotron Road

Berkeley, CA 94720, USA

Abstract

We analyze the reaction dynamics of central Pb+Pb collisions at 160 GeV/nucleon. First we estimate the energy density ϵ pile-up at mid-rapidity and calculate its excitation function: ϵ is decomposed into hadronic and partonic contributions. A detailed analysis of the collision dynamics in the framework of a microscopic transport model shows the importance of partonic degrees of freedom and rescattering of leading (di)quarks in the early phase of the reaction for $E_{lab} \geq 30$ GeV/nucleon. The energy density reaches up to 4 GeV/fm^3, 95% of which are contained in partonic degrees of freedom. It is shown that cells of hadronic matter, after $t \approx 2R/\gamma v_{cm}$, can be viewed as nearly chemically equilibrated. This matter never exceeds energy densities of ~ 0.4 GeV/fm^3, i.e. a density above which the notion of separated hadrons loses its meaning. The final reaction stage is analyzed in terms of hadron ratios, freeze-out distributions and a source analysis for final state pions.

---

[1]Feodor Lynen Fellow of the Alexander v. Humboldt Foundation

[2]Alexander v. Humboldt Fellow

The study of relativistic heavy ion collisions offers the unique opportunity to study hot and dense QCD matter under conditions which are thought to have existed in the early stages of our universe. However, only the hadronic final state of the heavy ion collision is accessible via experiment, or – in the case of leptonic probes – the time integral of the emission over the entire reaction history. Microscopic transport models offer the unique opportunity to link this final state information to the experimentally inaccessible early and intermediate reaction stages. In this paper we analyze the reaction dynamics of central Pb+Pb collisions at CERN/SPS energies. We focus specifically on the time evolution of energy density and its interpretation in terms of hadronic and partonic degrees of freedom. We then discuss the possible formation of a thermally and chemically equilibrated state in the central reaction zone and finally investigate the late reaction stages with a decomposition of freeze-out radii and sources for individual hadron species.

The determination of energy densities in ultra-relativistic heavy-ion collisions is crucial for any discussion involving a possible deconfinement phase transition to a QGP [1, 2, 3, 4, 5, 6, 7]. Estimates for the energy density during the hot and dense early reaction stage have been given by a large variety of different models [8, 5, 6, 9, 4, 10].

It has been questioned whether hadronic transport models are still valid at CERN/SPS energies: the energy density estimates obtained in these frameworks are claimed to be well above the critical energy density estimates for a deconfinement phase transition given by Lattice Gauge Theory [11, 12, 13]. Hadronic transport models, however, contain implicit partonic degrees of freedom – particle production at high energies is e.g. modeled via the production and fragmentation of strings [14, 15, 16].

In the UrQMD model used below, the leading hadrons of the fragmenting string contain the valence-quarks of the original excited hadron. These leading hadrons are allowed – in the model – to interact even during their formation time, with a reduced cross section, thus accounting for the original valence quarks contained in that hadron. Those leading hadrons represent a simplified picture of the leading (di)quarks of the fragmenting string. Newly to-be-produced hadrons which do not contain string valence quarks do in the present model not interact during their formation time – however, they contribute to the energy density of the system. A proper treatment of the partonic degrees of freedom during the formation time ought to include soft and hard parton scattering [28] and the explicit time-dependence of the color interaction between the expanding quantum wave-packets [25]: However, such an improved treatment of the internal hadron dynamics has not been implemented for light quarks into the present model. Therefore, in the following analysis all contributions stemming from hadrons within their formation time are termed "partonic". All contributions stemming from fully formed hadrons are termed "hadronic". The main focus of this paper is on the partitioning and the time evolution of the energy density and the collision dynamics of the early, intermediate, and late reaction stage at energies $E_{lab} = 10 - 200$ GeV/nucleon.

The UrQMD model [17] is based on analogous principles as (Relativistic) Quantum Molecular Dynamics [18, 19, 20, 21, 22]. Hadrons are represented by Gaussians in phase space and are propagated according to Hamilton's equation of motion. The collision term of the UrQMD model treats 55 different isospin (T) degenerate baryon (B) species (including nucleon-, delta- and hyperon- resonances with masses up to 2 GeV) and 32 different T-degenerate meson (M) species, including (strange) resonances as well as their corresponding anti-particles, i.e. full baryon-antibaryon symmetry is included. Isospin is treated explicitly. For hadronic excitations with masses $m > 2$ GeV (B) and > 1.5 GeV (M) a string model is used. Particles produced in the string fragmentation are assigned a formation time. This time τ_f physically consists of a quantal time τ_Q, i.e. before the partons are produced, $\tau_Q \sim 1/m$,
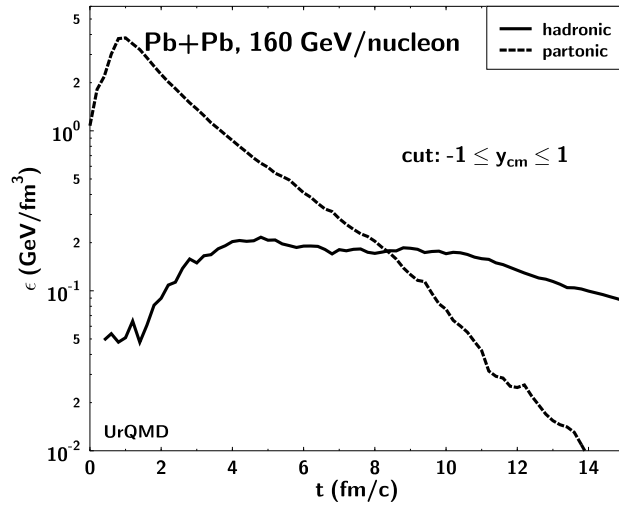
Figure 1: Time evolution of the energy density ϵ in central Pb+Pb reactions at 160 GeV/nucleon. ϵ has been decomposed into "partonic" and "hadronic" contributions and only particles around mid-rapidity have been taken into account. The early and intermediate reaction stages are dominated by the "partonic" contribution.

and a quantum diffusion time, τ_D, during which the partons evolve in the medium to build up their internal asymptotic wave-functions to form the hadron. τ_Q and τ_D differ for different parton and hadron species. For our present purpose, we – for the sake of simplicity – just collect all partons, formed and unformed, as one species. For a detailed overview of the elementary cross sections and string excitation scheme included in the UrQMD model, see ref. [17].

The partitioning of the distinct constituents can be inspected in Figure 1 which shows the time-evolution of the energy density for central Pb+Pb collisions at 160 GeV/nucleon. The nuclei are initialized such that they touch a $t = 0$ fm/c. The energy density is partitioned into the above defined "hadronic" contribution, from fully formed hadrons, and the "partonic" contribution, from partons, constituent quarks and diquarks within the hadron formation time. Nearly all incident baryons are rapidly excited into strings. Subsequently, "partonic" energy density builds up, reaching values of 4 GeV/fm^3 around midrapidity, $\Delta y = 1$ (at $t \approx 1$ fm/c). In the course of the reaction hadrons are formed which increases in the "hadronic" energy density, accompanied by a nearly exponential decrease in the "partonic" energy density.

These energy densities are calculated as follows: In the UrQMD model hadrons are represented by Gaussian wave packets. The width of the Gaussians $\sigma = 1.04$ fm and their normalization are chosen such that a calculation of the baryon density in the initial nuclei yields ground state nuclear matter density. The (energy-) densities in the central reaction zone are obtained by summing analytically over all Gaussian hadrons around mid-rapidity ($y_{c.m.} \pm 1$) at the locations of these hadrons and then averaging over these energy densities. This summation over Gaussians yields a smooth estimate for baryon- and energy-densities, as compared to counting hadrons in a test volume. The rapidity cut insures that only those particles are taken into account which have interacted. Thus, the free streaming "spectator" matter is discarded.

The absolute value of the energy density, however, may depend on the rapidity cut: Without rapidity cut the energy densities during the early reaction stage ($t \approx 1$ fm/c) can be as high as 20 GeV/fm^3. Even higher values in ϵ can be obtained by choosing the geometric center of the collision
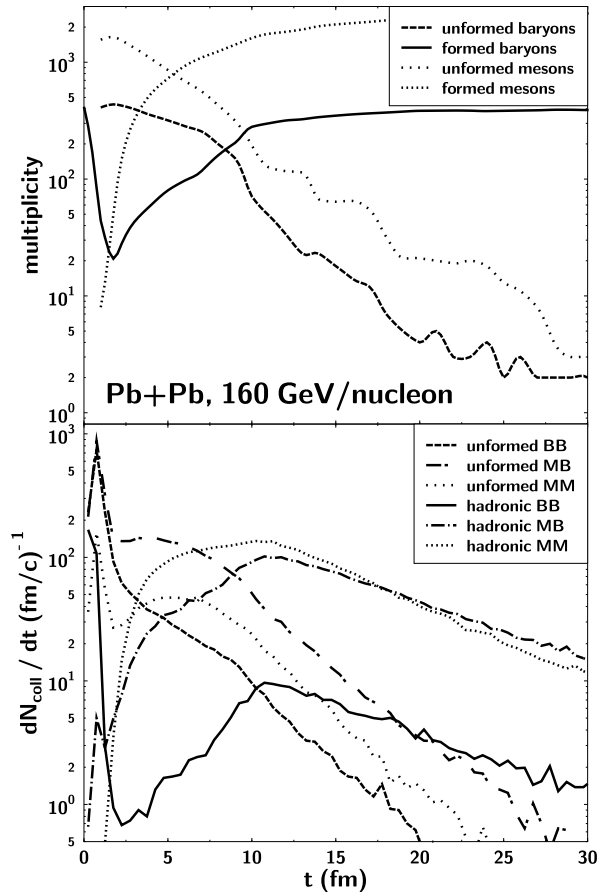
Figure 2: Top: Time evolution of the multiplicity of hadrons and partonic constituents, divided into baryonic and mesonic contributions. Bottom: Collision rates for baryon-baryon (BB) and meson-meson (MM) collisions. The rates have been decomposed into interactions involving formed hadrons and those involving partonic constituents.

for the sum over the Gaussians instead of averaging over the energy densities at the locations of the hadrons. The energy density at a single point may not be physically meaningful and therefore the latter method is favorable.

The time evolution of partonic constituents and hadrons is shown in the upper frame of figure 2. The first 5 fm/c of the reaction are dominated by the partonic constituents. The long-dashed and the dotted curves show the number of baryons and mesons contained in those constituents. In the case of leading-particles these can be interpreted as constituent (di)quarks or, for freshly born partons with small cross sections, as excitation modes of the color field.

The lower frame of figure 2 shows the time evolution of the number of baryon-baryon (BB) and meson-meson (MM) collisions, both for "hadronic" and "partonic" interactions. "Partonic" interactions denote interactions of *leading* (di)quarks either among themselves or with fully formed hadrons. The early reaction stages, especially the MM case, is clearly dominated by those "partonic" interactions. This number increases further if the scattering of the newly formed partons is included. Thus "partonic" degrees of freedom significantly contribute both, to the energy density, as well as to the collision dynamics in the first 5 fm/c.

It should be noted that the "partonic" collision rates can increase with the partonic cross section during formation time: In this analysis all interactions during formation time have been considered
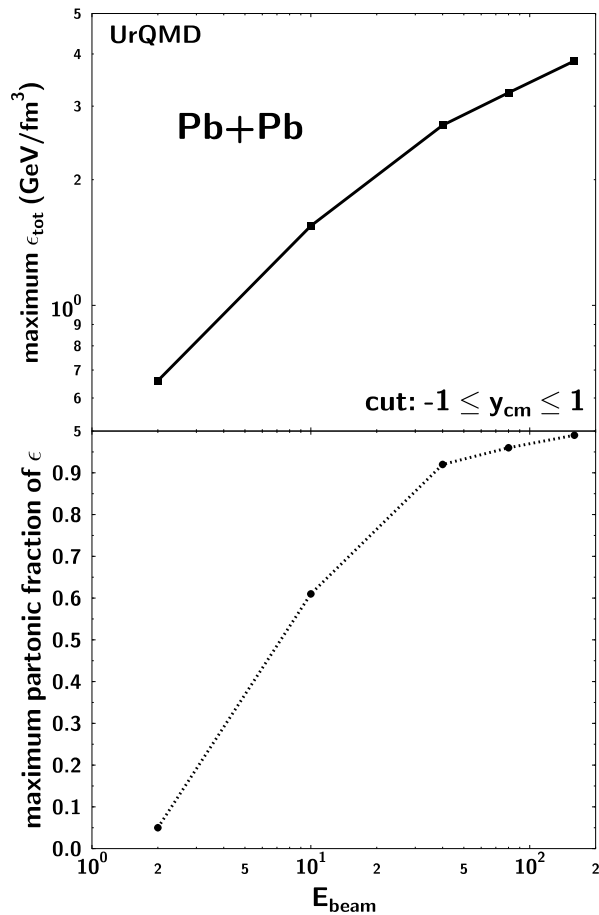
Figure 3: Top: excitation function of the maximum total energy density mid-rapidity hadrons experience. Bottom: excitation function of the maximum "partonic" fraction of energy density. Already at a beam energy of 40 GeV/nucleon more than 90% of the energy density is contained in partonic degrees of freedom at one time during the collision.

purely "partonic". Other scenarios, however, include a "hadronic" contribution to the cross section which increases continuously during τ_D and reaches its full hadronic value at the end of τ_D [25].

Do "partonic" degrees of freedom play any role at 10 GeV/nucleon, i.e. at the AGS? The upper frame of figure 3 shows the maximum total energy density obtained in central collisions of heavy nuclei as a function of incident beam energy, starting from 2 GeV/nucleon and going up to 200 GeV/nucleon. The energy density is obtained by the same method as used figure 1. However, here "partonic" and "hadronic" contributions have been summed. ϵ increases monotonously with the beam energy, reaching values as high as $4\,\mathrm{GeV/fm^3}$ for SPS energies, which would seem unreasonably high, if a purely hadronic scenario were used.

The lower frame of figure 3 shows the maximum fraction of the energy density which is contained in "partonic" degrees of freedom. Even at AGS, energies already more than half of the energy density is due to such "partonic" degrees of freedom, even though these do not yet dominate the "hadronic" contributions. At 40 GeV/nucleon, the maximum of the fraction of "partonic" energy density is already > 90% of the total ϵ.

The monotonous increase of the energy density excitation function does not imply that the excitation function of the space-time volume of high *baryon density* shows the same behavior. At AGS energies, $E_{lab} \sim 10$ GeV/nucleon, baryons still dominate the composition of the hadronic mat-
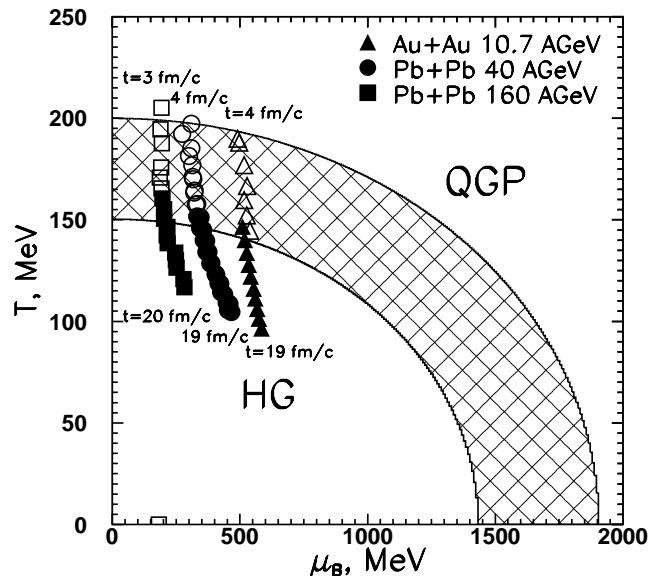
Figure 4: Temperature versus baryonic chemical potential predicted by the statistical model for the time evolution of the hadronic characteristics $\{\varepsilon,\ \rho_B,\ \rho_S\}$ obtained within UrQMD in the central cell ($2 \times 2 \times 1$ fm^3 cell) of central A+A collisions at 10.7, 40 and 160 GeV/nucleon. the open symbols show the non-equilibrium stage of the reaction, whereas the full symbols denote the phase of local thermal equilibrium in the central cell. The two solid lines correspond to the phase-boundary between a confined and deconfined phase calculated for two different bag constants, $B^{1/4} = 227$ and 302 MeV corresponding to T_c=150 and 200 MeV at $\mu_B = 0$.

ter, whereas at CERN/SPS energies, 200 GeV/nucleon, mesons constitute the largest fraction of the hadronic matter. The maximum space-time volume of dense *baryonic* matter can be reached at beam energies around 40 GeV/nucleon. A detailed analysis of that regime, also with respect to experimental signatures, is presently underway [26].

The time evolution of temperature T versus baryonic chemical potential μ_B for Au+Au reactions at 10.6 GeV/nucleon and Pb+Pb reactions at 40 and 160 GeV/nucleon, respectively, is plotted in figure 4. The thermodynamic quantities T and μ_B have been extracted by fitting a statistical model to the quantities energy-, baryon- and strangeness density $\{\varepsilon,\ \rho_B,\ \rho_S\}$ obtained from UrQMD in the central cell ($2 \times 2 \times 1$ fm^3 cell) of the heavy-ion reaction [23]. Here, the densities are calculated by summing over all relevant partonic and hadronic degrees of freedom in the cell. We see that the average μ_B in the reaction drops drastically with the initial collision energy, while the maximal temperature is growing and practically reaches the upper phase transition boundary with the critical temperature of T_c=200 MeV, as calculated with the MIT bag model (details of the used bag model can be found in [24]). However, during the early reaction stages matter in the central reaction cell is neither fully hadronic, nor thermally and chemically equilibrated. A detailed analysis of velocity distributions and particle spectra in the central cell [23] reveals that at approximately $t = 2$ fm/c the velocity distributions of nucleons become isotropic in the central cell. Pions, however, kinetically equilibrate much later, at $t \cong 8$ fm/c. This effect is caused by the non-zero formation time for non-leading particles. Full local thermal equilibrium (LTE) in the central cell (i.e. consistency of the particle spectra and yields with T and μ_B extracted from $\{\varepsilon,\ \rho_B,\ \rho_S\}$) is first reached at $t \cong 10$ fm/c. To distinguish the later fully equilibrated phase from the earlier reaction stage in which only nucleons show kinetic equilibrium, the statistical model fits to the early reaction stage are denoted by open symbols whereas the fits during
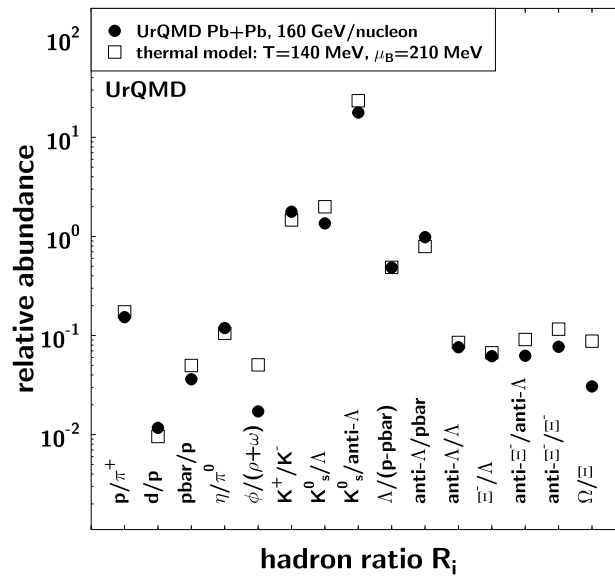
Figure 5: UrQMD prediction for hadron ratios in Pb+Pb collisions at midrapidity (full circles). The open squares denote a thermal model fit to the UrQMD calculation. The fit yields a temperature of T=140 MeV and a chemical potential of $\mu_B = 210$ MeV.

the LTE phase are shown in full symbols. During the phase of LTE energy densities of ~ 350 MeV/fm^3 are never exceeded, i.e. a density above which the notion of separated hadrons would lose its meaning. However, the main thermodynamic characteristics of the cell, T and μ_B change rapidly with time. This clearly demonstrates that a fireball type description of hadronic matter is inadequate.

Let us now turn to the hadronic final state of the heavy-ion reaction. Figure 5 shows a UrQMD prediction for hadron ratios in central Pb+Pb reactions at 160 GeV/nucleon around mid-rapidity (full circles). The UrQMD prediction has been fitted with a statistical model, yielding a temperature of T=140 MeV and a chemical potential of $\mu_B = 210$ MeV. However, this fit has been applied to the final hadron ratios after freeze-out. Here, the underlying assupmtion of the statistical model – namely a state of (global) equilibrium – is not anymore valid, since the break-up of the system and its freeze-out is governed by differences in the interaction properties (i.e. cross sections) of the individual hadron species.

To study the breakup of the system in greater detail, let us turn to freeze-out distributions for individual hadron species: Figure 6 shows the freeze-out time distribution for pions, kaons, antikaons and hyperons at mid-rapidity in central Pb+Pb reactions at 160 GeV/nucleon. The distributions have been normalized in order to compare the shapes and not the absolute values. In contrast to the situation at 2 GeV/nucleon, where each meson species exhibits distinctly different freeze-out time distributions [17], all meson species here show surprisingly similar freeze-out behavior – the freeze-out time distributions all closely resemble each other. Only the hyperons show an entirely different freeze-out behavior – the situation is even more extreme in the case of the multi-strange Ω, which exhibits a very sharp freeze-out time distribution, distinctly different from all other hadron species [23]. Whereas the common freeze-out characteristics of the mesons seem to hint at least at a partial thermalization, the hyperons show that even at SPS energies there exists no common global freeze-out for all hadron species. The same observation applies also to the distribution of transverse freeze-out radii. Since these distributions have a large width, the average freeze-out radius clearly does not define a freeze-out volume and therefore estimates of the reaction volume or energy density based on
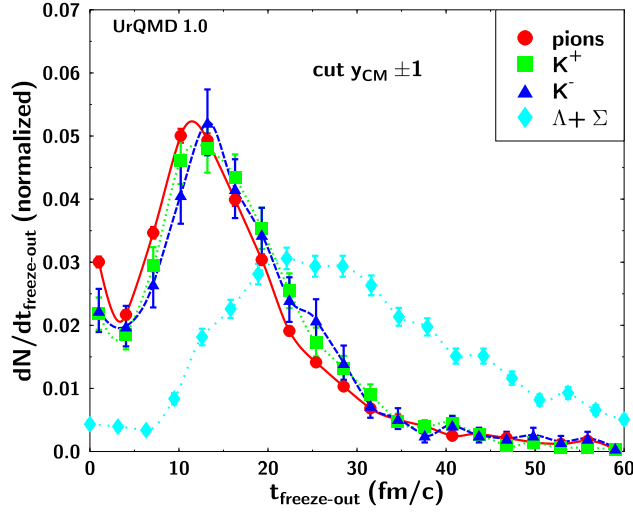
Figure 6: Normalized freeze-out time distribution for pions, kaons, antikaons and hyperons. As with the freeze-out radii, the times for the meson species are very similar. The hyperons again show a different behavior.

average freeze-out radii have to be regarded with great scepticism. The large width of the freeze-out distributions is supported experimentally by HBT source analysis which indicate the emitting pion source to be "transparent", emitting pions from everywhere rather than from a thin surface layer [30].

Figure 7 displays the respective sources from which negatively charged pions freeze-out. Only inelastic processes have been taken into account. Approximately 80% of the pions stem from resonance decays, only about 20% originate from direct production via string fragmentation. Elastic meson-meson or meson-baryon scattering adds a background of 20% to those numbers, i.e. 20% of all pions scatter elastically after their last inelastic interaction before freeze-out. The decay contribution is dominated by the ρ, ω and k^* meson-resonances and the Δ_{1232} baryon-resonance – no weak decays have been taken into account in this analysis. However, more than 25% of the decay-pions originate from a multitude of different meson- and baryon-resonance states, some of which are shown on the l.h.s. of figure 7; e. g. the two contributions marked ρ^* stem from the ρ_{1435} and the ρ_{1700}, respectively.

The analysis of the pion sources is of great importance for the understanding of the reaction dynamics and for the interpretation of HBT correlation analysis results. The 20% contribution of pions originating from string fragmentation is clearly non-thermal, since string excitation is only prevalent in the most violent, early reaction stages.

In summary, we have studied the evolution of relativistic Pb+Pb reactions at CERN/SPS energies from the early non-equilibrium phase through a stage of local thermal equilibration (in the central reaction cell) up to its final hadronic freeze-out. The importance of "partonic" degrees of freedom in the early reaction stage does not imply that an equilibrated Quark-Gluon-Plasma has been formed. In the UrQMD approach the "partonic" phase has been modeled as an incoherent superposition of non-interacting partonic constituents. Furthermore, these "partons" retain their original correlation into hadrons – deconfinement is not implemented into the present UrQMD approach. The leading (di)quark interactions (among each other and with fully formed hadrons) constitute an interacting "mixed phase" (for the constituent parton dynamics in this model, see, however [25, 27]). In contrast, parton cascades [28, 29] allow for interactions among the partons only, while hadronic final state
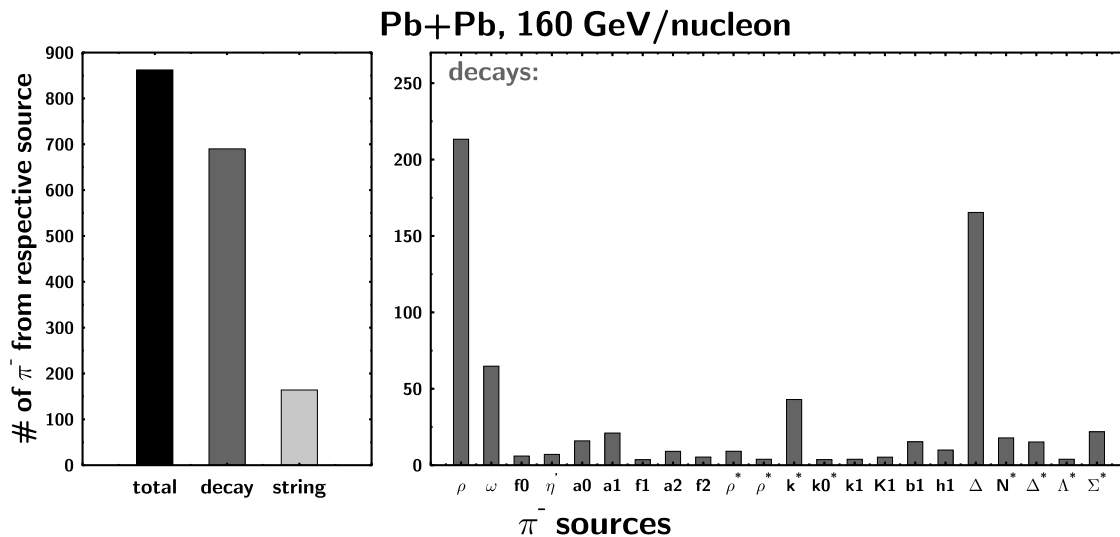
Figure 7: Pion sources in central Pb+Pb collisions at CERN energies: 80% of the final pions stem from resonance decays and 20% from direct production via string fragmentation. Decay-pions predominantly are emitted from the ρ and ω mesons and the Δ_{1232} resonance.

interactions are to a large extent neglected.

In the intermediate reaction phase, matter in the central cell can be viewed as hadrochemically equilibrated and exhibits an isentropic expansion. However, this equilibrium stage is limited only to the central reaction cell and breaks up in the late, dilute reaction phase close to freeze-out. The freeze-out of the system, which is governed by the individual hadron properties, has been studied in terms of freeze-out radii for different hadron species and a source analysis for the contributions of different microscopic processes to the final pion yield. A complex freeze-out scenario emerges with species- and momentum dependent broad freeze-out radius and time distributions.

References

[1] J. C. Collins and M. Perry, Phys. Rev. Lett. **34**, 1353 (1975).

[2] H. Stöcker, G. Graebner, J.A. Maruhn and W. Greiner, Phys. Lett. **B95**, 192 (1980).

[3] E. V. Shuryak, Phys. Rep. **61**, 71 (1980).

[4] L. McLerran, Rev. Mod. Phys. **58**, 1021 (1986).

[5] H. Stöcker and W. Greiner, Phys. Rep. **137**, 277 (1986).

[6] R. R. Clare and D. Strottman, Phys. Rep. **141**, 179 (1986).

[7] K. Kajantie and L. McLerran, Ann. Rev. Nucl. Part. Sci. **37**, 293 (1987).

[8] J. D. Bjorken, Phys. Rev. **D27**, 140 (1983).

[9] L. van Hove. Phys. Lett. **B118**, 138 (1982).

[10] M. Bleicher, L. Gerland, S.A. Bass, M. Brandstetter, C. Ernst, S. Soff, H. Weber, H. Stöcker and W. Greiner, Nucl. Phys. **A638**, 391, (1998).

[11] T. Blum, L. Kärkkäinen, D. Toussaint, and S. Gottlieb, Phys. Rev. **D51**, 5153 (1995).

[12] G. Boyd *et al.*, Phys. Rev. Lett. **75**, 4169 (1995).

[13] E. Laermann, Nucl. Phys. **A610**, 1c (1996).

[14] B. Andersson, G. Gustavson, and B. Nilsson-Almquist, Nucl. Phys. **B281**, 289 (1987).

[15] B. Andersson *et al.*, Comp. Phys. Comm. **43**, 387 (1987).

[16] T. Sjoestrand, Comp. Phys. Comm. **82**, 74 (1994).

[17] S. A. Bass, M. Belkacem, M. Bleicher, M. Brandstetter, L. Bravina, C. Ernst, L. Gerland, M. Hofmann, S. Hofmann, J. Konopka, G. Mao, L. Neise, S. Soff, C. Spieles, H. Weber, L. A. Winckelmann, H. Stöcker, W. Greiner, C. Hartnack, J. Aichelin and N. Amelin. Prog. Part. Nucl. Phys. **41**, 225 (1998), nucl-th/9803035.

[18] G. Peilert, A. Rosenhauer, H. Stöcker, W. Greiner, and J. Aichelin, Modern Physics Letters **A3**, 459 (1988).

[19] C. Hartnack, L. Zhuxia, L. Neise, G. Peilert, A. Rosenhauer, H. Sorge J. Aichelin, H. Stöcker and W. Greiner, Nucl. Phys. **A495**, 303 (1989).

[20] J. Aichelin, Phys. Rep. **202**, 233 (1991).

[21] H. Sorge, H. Stöcker, and W. Greiner, Ann. Phys. **192**, 266 (1989).
     H. Sorge, Phys. Rev. **C52**, 3291 (1995).

[22] E. Lehmann, R. Puri, A. Faessler, G. Batko, and S. Huang, Phys. Rev. **C51**, 2113 (1995).

[23] L.V. Bravina, M. Brandstetter, M.I. Gorenstein, E.E. Zabrodin, M. Belkacem, M. Bleicher, S.A. Bass, C. Ernst, M. Hofmann, S. Soff, H. Stöcker and W. Greiner. J. Phys. **G** in print, nucl-th/9810036.

[24] M.I. Gorenstein, H. Stöcker, G.D. Yen, S.N. Yang and W. Greiner. J. Phys. **G24**, 1777 (1998).

[25] L. Gerland, L. Frankfurt, M. Strikman, H. Stöcker, and W. Greiner, Phys. Rev. Lett. **81**, 762 (1998).

[26] H. Weber, S.A. Bass, M. Bleicher, C. Spieles, H. Stöcker and W. Greiner, to be published.

[27] C. Spieles, L. Gerland, N. Hammon, M. Bleicher, S.A. Bass, H. Stoecker, W. Greiner, C. Lourenco and R. Vogt, Euro. Phys. J. **A1**, 51 (1998).

[28] K. Geiger and B. Müller, Nucl. Phys. **B369**, 600 (1992).

[29] K. Geiger, Comput. Phys. Commun. **104**, 70 (1997), hep-ph/9701226.

[30] G. Roland *et al.* Nucl. Phys. **A638**, 91 (1998).
     U. Heinz, Nucl. Phys. **A638**, 357 (1998).